Transient and steady state investigation of selective and non-selective reaction pathways in the oxidative dehydrogenation of propane over supported vanadia catalysts

Evgenii V. Kondratenko,* Norbert Steinfeldt and Manfred Baerns

Received 2nd November 2005, Accepted 16th January 2006
First published as an Advance Article on the web 2nd February 2006
DOI: 10.1039/b515603n

Mechanistic aspects of the formation of C_3H_6, CO and CO_2 in the oxidative dehydrogenation of propane over VO_x/γ-Al_2O_3 materials have been investigated by means of steady state and transient isotopic tests. The materials possessed highly dispersed and polymerised VO_x species as well as bulk-like V_2O_5. Propene was primarily formed *via* oxidative dehydrogenation of propane by lattice oxygen of VO_x species. It was suggested that non-selective consecutive propene oxidation is initiated by the breaking of the C–C bond in the molecule by the lattice oxygen, forming formaldehyde as a side product, which is further oxidised to CO and CO_2. The following order of initial steady state propene selectivity (at a zero degree of propane conversion) as a function of the nature of VO_x species was established: a mixture of bulk-like V_2O_5 and polymerised VO_x > polymerised VO_x > highly dispersed VO_x species. The low propene selectivity over highly dispersed VO_x species was explained by the fact that these species do not fully cover the bare acidic surface of γ-Al_2O_3 where propene adsorption and further oxidation take place. Thus, two different locations of CO_x formation were considered: (i) in the vicinity of acidic sites of the support and (ii) on VO_x species. The propene selectivity over samples possessing polymerised VO_x species and bulk-like V_2O_5 strongly decreased with an increasing degree of propane conversion. Contrarily, highly dispersed VO_x species showed the lowest ability for consecutive propene oxidation.

1 Introduction

During the last fifteen years the selective oxidation of light alkanes to their olefins or to other higher-valued products (aldehydes, ketones, carboxylic acids, epoxides *etc*.) has attracted both industrial and scientific attention due to the abundance of light alkanes and the potential for developing innovative lower cost processes.[1–4] Oxidative transformations of propane are of particular importance because propane is a component of natural gas, which may eventually be considered as a preferable raw material, substituting naphtha from crude oil. For the oxidative dehydrogenation of propane (ODP) to propene, supported vanadium-based catalytic materials have been reported to be among the most active and selective.[1,5,6] Unfortunately, with present day catalytic materials high selectivities towards propene are mostly achieved only at low degrees of propane conversion due to the higher reactivity of propene compared to propane. This gives rise to a fundamental problem of activation of lower reactive alkanes in the presence of more reactive reaction products. Therefore, the catalytic material should selectively convert the alkane molecule without further oxidation of propene. This situation results in the need to kinetically isolate the selective reaction products before side products are formed. The extent of kinetic isolation of the selective products depends on the relative rates of formation of a specific selective product and its rates of further conversion to the side products.

For the ODP reaction, different physico-chemical properties of supported vanadium-containing materials such as reducibility, acidity and basicity, coordination geometry and the dispersion of VO_x species have been identified as being important factors affecting catalytic performance.[2,7–16] A better understanding of the relationship between the kinetics and mechanism of the ODP reaction on one hand and physico-chemical properties of catalytic materials on the other hand would possibly allow one to control the overall process of propane conversion and, hence, to provide useful guidelines for an improved rational catalyst design. Although the physico-chemical properties of catalytic materials have been extensively studied, only a few studies related these properties to mechanistic aspects of the ODP reaction.[17–21] These studies proved that C_3H_6 formation occurs *via* a Mars–van Krevelen mechanism, but none of them gave a detailed mechanistic understanding of CO_x formation. Generally, CO_x products are formed *via* propane or propene oxidation by lattice and adsorbed oxygen species.[17,21–23] Bielanski and Haber[24] have tentatively suggested a detailed mechanistic scheme of alkenes transformation to CO_x with the participation of adsorbed and lattice oxygen species. Alkenes are activated by oxygen species at the double bond giving saturated aldehydes, which are further oxidised to CO_x. Based on the analysis of a kinetic

Leibniz-Institut für Katalyse e. V. an der Universität Rostock, Aussenstelle Berlin†, Richard-Willstätter-Str. 12, D-12489 Berlin, Germanyevgenii@aca-berlin.de; Fax: +49 30 63924454; Tel: +49-30-63924448
† *Formerly Institute for Applied Chemistry Berlin-Adlershof*

isotopic effect in the ODP reaction over V_2O_5(10 wt%)/ZrO_2, Chen *et al.*[25] have recently claimed the presence of two different lattice oxygen species, which participate in selective dehydrogenation and non-selective combustion reactions. However, these authors did not discuss any mechanistic details of the CO and CO_2 formation.

Compared to steady state experiments, transient techniques have the potential to provide considerably more mechanistic insights into individual steps of catalytic reactions. Therefore, the temporal analysis of products (TAP) reactor in combination with steady state ambient pressure catalytic tests was applied for investigating selective and non-selective routes of the ODP reaction over VO_x/γ-Al_2O_3 materials possessing differently structured VO_x species. The main aim of the present contribution was to elucidate the nature of the active catalytic sites required for both selective and non-selective transformations of propane. In order to identify common factors influencing selectivity and activity of the studied catalysts in the ODP reaction, mechanistic insights into oxygen, propane and propene activation will be related to physico-chemical properties of VO_x/γ-Al_2O_3 materials. The materials have been previously characterised by our group[26,27] using various characterisation methods (BET, EPR, XRD, electrical conductivity, NMR and *in situ* UV/Vis-DRS spectroscopies as well as H_2-TPR).

2 Experimental

2.1 Catalyst preparation

V_2O_5 (Merck), γ-Al_2O_3 (Degussa) and boehmite (Disperal, Condea) were used for catalyst preparation. The required amount of V_2O_5 was dissolved in oxalic acid at 348 K followed by the addition of 1 g of polyvinyl alcohol (PVA) whilst stirring until the solution became clear. The same amounts of boehmite and γ-Al_2O_3 (2 or 4 g) were then added to the solution with continuous stirring. Boehmite and PVA were added for the homogeneous distribution of the vanadia on the catalyst surface.[26,27] Water was evaporated from the resulting mixture at 333 K for 12 h followed by calcination in the temperature range from 773–973 K for 6 h in air.

2.2 Catalyst characterisation

As pointed out in the Introduction, all catalytic materials have previously been characterised with the aim to determine the nature and distribution of VO_x species as well as their reducibility and reoxidation. The most relevant results are summarised in Table 1. Inductively coupled plasma-optical emission spectrometry was used to determine the vanadium content after catalyst calcination. The exact vanadium concentrations and calcination temperatures are also listed in Table 1 inside brackets in the catalyst formula.

2.3 Steady state catalytic testing

Catalytic measurements were carried out in a U-type fixed bed reactor made of quartz (id = 6 mm) at ambient pressure. Catalyst particle size was between 255–450 μm. The feed consisted of 15 vol% oxygen and 30 vol% propane in nitrogen; the latter gas was used as the internal standard for gas chromatographic product analysis (HP-5890 or μ-GC equipped with Poraplot Q and Molsiev 5 columns). For acquiring selectivity data at different degrees of propane conversion, the residence time was varied by using different amounts of catalyst and total flow rates. The reaction temperature was varied between 613–803 K. For an estimation of initial rates of propene formation (eqn (1)) and propane consumption (eqn (2)), the degree of propane conversions was kept below 4%.

$$r_{C_3H_6} = \left(\frac{F_t}{22\,400A}\right)\left(\frac{C(C_3H_6)}{100}\right) \quad (1)$$

$$r_{C_3H_8} = \left(\frac{F_t}{22\,400A}\right)\left(\frac{(C(C_3H_6) + \frac{1}{3}C(CO) + \frac{1}{3}C(CO_2))}{100}\right) \quad (2)$$

In these equations, A is $m_{cat}S_{cat}$ and m_V for the rates related to the specific surface area and to the total vanadium content, respectively. F_t is the total volumetric flow (mL(STP) min^{-1}), m_{cat} is the catalyst mass (g), $C(C_3H_6)$, C(CO) and $C(CO_2)$ are the C_3H_6, CO and CO_2 concentrations at the reactor outlet (vol%), S_{cat} is BET surface area (m^2 g^{-1}) and m_V is the total vanadium mass per gram of catalyst.

2.4 Transient catalytic experiments

The TAP-2 reactor system has been comprehensively described elsewhere.[28] The catalyst (sieve fraction 250–350 μm) was packed into the micro-reactor made of quartz (40 mm length and 6 mm id) between two layers of quartz of the same particle size. The amount of catalyst was varied between 30–150 mg. Before each experiment the catalyst was treated in a flow of O_2 (30 mL min^{-1}) at 873 K and ambient pressure for *ca.* 1 h. Hereafter, the micro-reactor was evacuated at 823 K to 10^{-5} Pa and the reactor temperature was set to the desired values (573–823 K). Pulses containing small amounts of reactants (1×10^{14}–5×10^{14} molecules per pulse) diluted by an inert gas were injected into the micro-reactor *via* two high speed valves. For such pulse sizes, gas transport through the reactor is in the Knudsen diffusion regime. This means that the transient responses are a function of gas–solid interactions and not influenced by collisions between gas phase molecules. Thus, heterogeneous reaction steps are under investigation. Three types of transient experiments were carried out:

- A gas mixture of a certain composition was pulsed into the reactor and transient responses were monitored at atomic mass units (AMUs) related to the feed components, reaction products and inert gas. The following reaction mixtures were used: C_3H_8 : Ne = 1 : 1, C_3H_6 : Ne = 1 : 1, $^{16}O_2$: Ne = 1 : 1, C_3H_8 : C_3H_6 : Ne = 10 : 1 : 10, $^{18}O_2$: Ne = 1 : 1 and CO : Ne = 1 : 1.
- $^{16}O_2$: Ne = 1 : 1 and C_3H_8 : Ne = 1 : 1 or $^{18}O_2$: Ne = 1 : 1 and C_3H_8 : Ne = 1 : 1 reaction mixtures were sequentially pulsed from two pulse valves with different time intervals (Δt = 0–1 s).
- Reducibility and related reactivity of differently structured VO_x species were determined by means of C_3H_8 multi pulse experiments. In these experiments, the catalytic materials were progressively treated by pulses containing a large number (*ca.*

Table 1 Surface and bulk characteristics of the $VO_x/\gamma\text{-}Al_2O_3$ samples used

Catalyst[a]	S_{BET}/ $m^2\ g^{-1}$	V content/ wt%	VO_x density/ V atoms nm^{-2}	Crystalline phases[b]	Main VO_x species[b]
$VO_x(1/973)/\gamma\text{-}Al_2O_3$	121	1	0.98	No	Tetrahedral highly dispersed
$VO_x(4.6/973)/\gamma\text{-}Al_2O_3$	48	4.6	11.3	V_2O_5	Tetrahedral polymerised
$VO_x(4.5/873)/\gamma\text{-}Al_2O_3$	136	4.5	3.9	No	Tetrahedral polymerised
$VO_x(9.5/973)/\gamma\text{-}Al_2O_3$	8.7	9.5	129	V_2O_5	Tetrahedral polymerised
$VO_x(8.9/873)/\gamma\text{-}Al_2O_3$	86	8.9	12.2	$AlVO_4$	Tetrahedral polymerised
$VO_x(8.9/773)/\gamma\text{-}Al_2O_3$	137	8.9	7.6	No	Tetrahedral and octahedral polymerised

[a] For example, $VO_x(1/973\ K)/\gamma\text{-}Al_2O_3$ means that the vanadium loading is 1 wt% and the calcination temperature is 973 K. [b] Based on UV/Vis, NMR and XRD analysis.[26,27]

10^{16}) of propane molecules. The amount of oxygen removed from the VO_x species was calculated from the amount of products formed, taking stoichiometry into account.

In the experiments, Ne (4.5), Xe (4.0), O_2 (4.5), $^{18}O_2$ (98% O atoms), C_3H_8 (3.5), C_3H_6 (3.5), and CO (3.5) were used. The $^{18}O_2$ oxygen isotope was purchased from ISOTEC. Transient responses were monitored using a quadruple mass spectrometer (HAL RC 301 Hiden Analytical). The following AMUs were used for the identification of the various compounds: 132 (Xe), 48 ($C^{18}O_2$), 46 ($C^{18}O^{16}O$), 44 ($C^{16}O_2$, C_3H_8), 42 (C_3H_8 and C_3H_6), 36 ($^{18}O_2$), 32 ($^{16}O_2$, $H_2C^{18}O$), 31 ($H_2C^{18}O$), 30 ($H_2C^{16}O$, $H_2C^{18}O$ and $C^{18}O$), 29 (C_3H_8, $H_2C^{16}O$), 28 (C_3H_8, $C^{16}O$ and $C^{16}O_2$), 20 (Ne), 18 ($H_2{}^{16}O$). The concentrations of feed components and reaction products were determined from the respective AMUs using standard fragmentation patterns and sensitivity factors. For each AMU pulses were repeated 10 times and averaged to improve the signal-to-noise ratio. The individual AMUs in multi-pulse experiments with C_3H_8 (pulse size is *ca.* 10^{16} molecules) were recorded without averaging.

3 Results and discussion

The results of physico-chemical characterisation as well as of steady state catalytic tests are summarised in the following two sections (3.1 and 3.2). Thereafter, mechanistic insights into C_3H_6 and CO_x formation from transient experiments in the TAP reactor are presented and discussed (section 3.3). Finally (section 3.4), a reaction scheme for the ODP reaction is suggested, which explains the influence of the alumina surface and the nature of the VO_x species (highly dispersed, polymerised VO_x species and bulk-like V_2O_5) on the selectivity–conversion relationships of the ODP reaction over $VO_x/\gamma\text{-}Al_2O_3$.

3.1 Effect of calcination temperature and vanadium loading on specific surface area and distribution of VO_x species

Since the results of our detailed physico-chemical characterisation analysis of $VO_x/\gamma\text{-}Al_2O_3$ materials have been published previously,[26,27] the most relevant results are briefly reported below. These data are the basis of the further elucidation of some mechanistic aspects. The specific surface areas of $VO_x/\gamma\text{-}Al_2O_3$ catalysts (Table 1) decrease with an increase in vanadium content and calcination temperature. The effect of calcination temperature on the specific surface area is stronger than that of the vanadium content. This is due to temperature-induced interactions between alumina and vanadia resulting in the formation of different phases ($AlVO_4$ and V_2O_5) and the blocking of pores.

Vanadium loading and calcination temperature also influence the apparent VO_x surface density (V nm^{-2} in Table 1), which was calculated according to ref. 15. The density values of 2.3 and 7.5 V nm^{-2} have been suggested for monovanadate and polyvanadate monolayers, respectively.[29] Blasco and López Nieto[2] have estimated a VO_x density of 10 V nm^{-2} corresponding to the vanadium monolayer for alumina-supported catalysts. Table 1 illustrates that highly dispersed, tetrahedrally coordinated VO_x species are stabilized on the surface of the $VO_x(1/973)/\gamma\text{-}Al_2O_3$ material even after catalyst calcination at 973 K. An increase in vanadium loading generally results in a transformation of highly dispersed VO_x species to polymerised species and the dispersion of VO_x species decreases. Polymerised VO_x surface species and crystalline vanadium-containing phases coexist in samples calcined at 873 K and high (>4.5 wt%) vanadium loadings (Table 1). The amount of vanadium in the crystalline phases increases with an increase in vanadium content and calcination temperature. In other words, the lower the calcination temperature, the higher the concentration of VO_x species on the surface in comparison to the crystalline phases ($AlVO_4$ and V_2O_5).

3.2 Steady state catalytic results

As expected, C_3H_6, CO and CO_2 were the main gas phase products over differently loaded $VO_x/\gamma\text{-}Al_2O_3$ catalytic materials in the whole temperature range from 613–803 K. The initial rates of propene formation and propane conversion, which are related to the total specific surface area of the catalytic materials (μmol $min^{-1}\ m^{-2}$) and to the total amount of vanadium (μmol $min^{-1}\ g_v^{-1}$), are presented in Table 2. An increase in the vanadium content leads to an increase in the rates related to the specific surface areas for samples calcined at the same temperature. The selectivity towards propene increases, too. However, the rates related to the total vanadium content have a maximum for $VO_x(4.6/873)/\gamma\text{-}Al_2O_3$ and $VO_x(8.9/773)/\gamma\text{-}Al_2O_3$ (Table 2). The lower rate over $VO_x(1/973)/\gamma\text{-}Al_2O_3$ (in comparison to the above samples) has to be particularly emphasized, because this sample only possesses the highly dispersed VO_x species. This finding indicates a dissimilarity in the reactivity of highly dispersed and polymerised VO_x species. The difference may be related to the fact that not all highly dispersed VO_x can participate in the ODP reaction. An explanation is given in section 3.3.3, which takes

Table 2 Catalytic performance of different vanadia-based catalytic materials in the oxidative dehydrogenation of propane ($C_3H_8 : O_2 : N_2 = 30 : 15 : 55$, $T = 613$ K)

Catalyst[a]	$S(C_3H_6)$ (%)	Rate/μmol min^{-1} m^{-2}		Rate/μmol min^{-1} g_V^{-1}	
		C_3H_8	C_3H_6	C_3H_8	C_3H_6
$VO_x(1/973)/\gamma\text{-}Al_2O_3$	63	7.36×10^{-2}	4.63×10^{-2}	891	560
$VO_x(4.6/973)/\gamma\text{-}Al_2O_3$	93	2.08	1.95	2172	2031
$VO_x(4.6/873)/\gamma\text{-}Al_2O_3$	88	0.78	0.69	2500	2200
$VO_x(9.5/973)/\gamma\text{-}Al_2O_3$	96	4.05	3.9	371	357
$VO_x(8.9/873)/\gamma\text{-}Al_2O_3$	79	2.45	1.97	2400	1900
$VO_x(8.9/773)/\gamma\text{-}Al_2O_3$	81	0.17	0.14	2700	2200

[a] For example, VO_x(1/973 K)/γ-Al_2O_3 means that vanadium loading is 1 wt% and calcination temperature is 973 K.

the reducibility of different VO_x species by propane into account. The lowest rate related to the total vanadium content was determined for $VO_x(9.5/973)/\gamma\text{-}Al_2O_3$. This is due to the fact that bulk-like V_2O_5 species are the main VO_x species over this sample (Table 1) and as such not all vanadium atoms are directly accessible for the ODP reaction.

For a detailed study of the influence of the structure and dispersion of VO_x species on product selectivities, catalytic tests were performed at different degrees of propane conversion. Fig. 1 compares selectivity–conversion plots of the ODP reaction over samples possessing VO_x species, which are (i) either highly dispersed, (ii) highly dispersed and polymerised or (iii) polymerised and bulk-like V_2O_5. From the selectivity–conversion plot for the $VO_x(1/973)/\gamma\text{-}Al_2O_3$ sample, which contains highly dispersed VO_x species, non-zero selectivities of CO, CO_2 and C_3H_6 can be expected upon extrapolation to the zero degree of propane conversion. The non-zero selectivities are an indication that all these reaction products are at least partly formed in parallel from propane. Highly dispersed VO_x species are gradually transformed to polymerised species and finally to bulk-like vanadium-containing phases upon increasing the content of vanadium on γ-Al_2O_3. Simultaneously, CO and CO_2 selectivities at the zero degree of propane conversion become lower compared to $VO_x(1/973)/\gamma\text{-}Al_2O_3$ (Fig. 1). This means that direct propane oxidation to CO_2 and CO is inhibited. The VO_x $(9.5/973)/\gamma\text{-}Al_2O_3$ sample, which contains both polymerised VO_x and bulk-like V_2O_5, has the highest initial propene selectivity and the lowest selectivity to CO_x at the zero degree of propane conversion. From the results of the catalyst characterisation in Table 1 (BET surface, vanadium content, VO_x surface density and phase composition) it can be expected that the alumina surface has been gradually covered by VO_x species with an increasing vanadium loading. Since γ-Al_2O_3 is an acidic support,[7] the differences obtained in the ODP performance between low and high loaded $VO_x/\gamma\text{-}Al_2O_3$ may be due to differences in acidic properties. The influence of support acidity on propene selectivity is discussed in detail below (section 3.4) taking into account the results on propene adsorption/desorption in section 3.3.4.

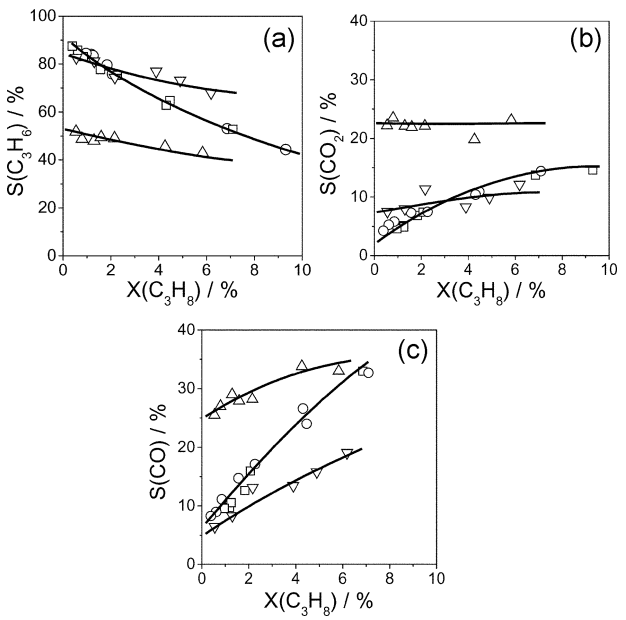

Fig. 1 Selectivity of (a) C_3H_6, (b) CO_2 and (c) CO determined at different degrees of propane conversion over $VO_x(1/973)/\gamma\text{-}Al_2O_3$ (Δ), $VO_x(4.6/873)/\gamma\text{-}Al_2O_3$ (▽), $VO_x(4.6/973)/\gamma\text{-}Al_2O_3$ (○) and $VO_x(9.5/973)/\gamma\text{-}Al_2O_3$ (□) ($T = 713$ K, $C_3H_8 : O_2 : N_2 = 30 : 15 : 55$).

Another important observation from the catalytic tests is the influence of propane conversion on product selectivities. For $VO_x(1/973)/\gamma\text{-}Al_2O_3$, C_3H_6 selectivity decreases slightly, while CO selectivity increases with an increasing degree of propane conversion (Fig. 1). This is an indication of consecutive reactions. Since CO_2 selectivity is nearly independent of propane conversion, C_3H_6 is mainly oxidised to CO. When vanadium loading increases, propane conversion strongly influences C_3H_6 selectivity and accompanied changes in CO and CO_2 selectivities (Fig. 1). For $VO_x(4.5/873)/\gamma\text{-}Al_2O_3$ and $VO_x(9.5/973)/\gamma$-Al_2O_3 possessing polymerised VO_x species and bulk-like V_2O_5, it is clear that CO and CO_2 are mainly formed *via* consecutive oxidation of propene. The highest decrease in propene selectivity with increasing degree of propane conversion was found for the samples which contain bulk-like V_2O_5. Based on the above discussion, differently structured VO_x species (highly dispersed, polymerised or bulk-like V_2O_5) perform differently in the ODP reaction over $VO_x/\gamma\text{-}Al_2O_3$. At this stage, it is not possible to conclude whether the differences are due to different oxygen species (terminal or bridging oxygen) in VO_x species. As stressed in section 3.4, the density of neighbouring oxygen species and the presence of bare γ-Al_2O_3 surface are possible factors influencing the catalytic performance.

3.3 Mechanistic analysis of transient studies

For a deeper understanding of the reactivity and selectivity of differently structured VO_x species and for the identification of

active oxygen species in the ODP reaction, transient experiments with C_3H_8, C_3H_6 and $^{18}O_2$ over selected VO_x/γ-Al_2O_3 materials were carried out in the TAP reactor. Particular attention was paid to CO and CO_2 formation and to factors determining the selectivity to propene as discussed in the following four subsections.

3.3.1 Reaction products of propane and propene oxidation by VO_x in the absence of gas phase oxygen. The interaction of C_3H_8 with differently loaded VO_x/γ-Al_2O_3 materials was studied in the temperature range of 773–823 K by means of C_3H_8 pulse experiments (section 2.4). C_3H_6, CO, CO_2, H_2O and formaldehyde were observed. H_2CO was identified using isotopically labelled VO_x species ($V^{18}O_x$). Since gas phase oxygen was not present in the C_3H_8 pulse, all of the reaction products were formed by C_3H_8 oxidation with lattice oxygen of the VO_x species. Typical transient responses of the observed carbon-containing products along with the response of unreacted propane are plotted in Fig. 2(a). From this figure it is clear that each transient response has a unique mean residence time, temporal maximum and decay. The transient response of C_3H_8 appears after the shortest time interval and has the fastest decay. The transient response of C_3H_6 is similar to that of C_3H_8 but it is slightly shifted to longer times. Formaldehyde was observed a short time after C_3H_6 and C_3H_8. Transient responses of CO and CO_2 are significantly shifted to longer times as compared to those of the previous gas phase reactants and have the broadest shape.

The shape of the transient responses and their order of appearance reveal important mechanistic and kinetic information on chemical and transport phenomena inside the reactor. The order of appearance of the reaction products in Fig. 2(a) can be interpreted in the following manner. Since the transient response of C_3H_6 follows that of C_3H_8 directly, it is concluded that the initial step of the ODP reaction is the formation of propene *via* the breaking of the C–H bonds in the propane molecule as reported previously.[25] The propene initially formed reacts further at the C–C bond yielding formaldehyde followed by its further oxidation to CO and CO_2. A similar idea was discussed by Bielanski and Haber[24] for the oxidation of alkenes over V_2O_5. However, they suggested that electrophilic species (O_2^-, O_2^{2-} or O^-) rather than lattice oxygen species participate in the breaking of the C–C bond in the alkene molecule. Our results show that the lattice oxygen of VO_x species is also active for C–C bond scission.

In order to prove whether the same side-reaction products seen for the reaction of propane are also formed from propene, low intensity pulses of propene were passed over VO_x/γ-Al_2O_3 catalysts at different temperatures (623–773 K). CO, CO_2 and H_2CO were again the only carbon-containing reaction products (Fig. 2(b)). The order of appearance of their transient responses is the same as that seen when pulsing propane (Fig. 2(a)). H_2CO appears directly after C_3H_6 followed by CO and CO_2. This observation supports the statement that formaldehyde is an intermediate product of propene oxidation to CO_x.

Additionally, it has to be emphasized that the degree of propene conversion was considerably higher than that of propane under the same conditions (Table 3). This agrees well with the higher reactivity of alkenes in comparison to the

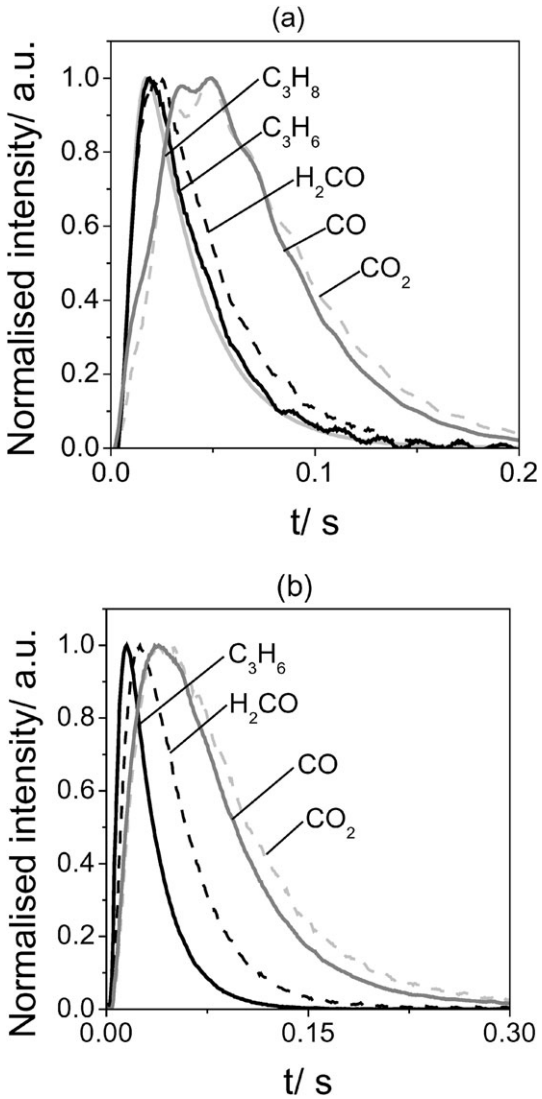

Fig. 2 Transient responses to pulsing (a) C_3H_8 and (b) C_3H_6 over VO_x (9.5/973)/γ-Al_2O_3 at 848 K.

respective alkanes. In order to check if C_3H_8 and C_3H_6 compete for the same active sites, a mixture of propane with propene (C_3H_8 : C_3H_6 : Ne = 10 : 1 : 10) was pulsed over the selected materials at different temperatures (773 and 798 K). Despite the fact that the C_3H_6 concentration in the feed mixture is *ca.* 10 times lower than that of C_3H_8, the degree of C_3H_6 conversion was considerably higher than that of C_3H_8. The degrees of propane conversion obtained upon single pulsing of C_3H_8 : Ne = 1 : 1 and C_3H_8 : C_3H_6 : Ne = 10 : 1 : 10 mixtures over VO_x(1/973)/γ-Al_2O_3 and VO_x(9.5/973)/γ-Al_2O_3 catalysts are shown in Fig. 3. VO_x(1/973)/γ-Al_2O_3 possesses isolated VO_x species, while polymerised VO_x and bulk-like V_2O_5 species are dominant in VO_x(9.5/973)/γ-Al_2O_3. For both samples, the degree of propane conversion is lower in the presence of propene than in its absence. Thus, the selective route of the ODP reaction, *i.e.* direct propane oxidation to propene, is inhibited in the presence of propene. In other words, propane and propene compete for the same active catalyst sites, *i.e.* lattice oxygen. Pulse experiments with a

Table 3 Propane and propene conversion over various catalytic materials upon pulsing C_3H_8/Ne = 1 and C_3H_6/Ne = 1 mixtures at 773 K. The pulse size of Ne is *ca.* 5×10^{14} molecules

Catalyst[a]	$X(C_3H_8)$/%	$X(C_3H_6)$/%	$X(C_3H_6)/X(C_3H_8)$
$VO_x(1/973)/\gamma\text{-}Al_2O_3$	23	86	3.7
$VO_x(4.6/973)/\gamma\text{-}Al_2O_3$	30	81	2.7
$VO_x(9.5/973)/\gamma\text{-}Al_2O_3$	7	47	6.7
$VO_x(4.5/873)/\gamma\text{-}Al_2O_3$	45	97	2.2
$VO_x(8.9/873)/\gamma\text{-}Al_2O_3$	33	84	2.5
$VO_x(8.9/773)/\gamma\text{-}Al_2O_3$	14	80	5.7

[a] For example, $VO_x(1/973\ K)/\gamma\text{-}Al_2O_3$ means that the vanadium loading is 1 wt% and the calcination temperature is 973 K.

C_3H_8–CO mixture and single CO pulsing give evidence that CO oxidation to CO_2 does not play any significant role in the ODP reaction over these materials in the temperature range applied.

3.3.2 Active oxygen species. The effect of lattice oxygen or adsorbed oxygen species on the ODP reaction was studied by sequentially pulsing O_2 : Xe = 1 : 1 and C_3H_8 : Ne = 1 : 1 mixtures with time delays (Δt) varying from 0–1 s. Such an operation enables one to understand if adsorbed oxygen species (formed in the O_2 pulse) influence the product distribution in the C_3H_8 pulse. Conversely, it can be seen whether carbon-containing surface intermediates, which are formed in the C_3H_8 pulse and are retained on the catalyst surface, are oxidized in the subsequent O_2 pulse. Reaction products were observed in the C_3H_8 pulse only. This finding is in contradiction to the recently reported results of a similar mechanistic study of the ODP reaction over VO_x(16 wt% V_2O_5)/γ-Al_2O_3 by Mul *et al.*[30] These authors observed CO_x formation in the O_2 pulse. This was considered by them to be an oxidation of carbon-containing species which were formed in the C_3H_8 pulse. The disagreement between the two studies may be due to the difference in experimental conditions. In the present study, the pulse size of C_3H_8 was *ca.* 0.5 nmol, while Mul *et al.* used larger pulse sizes. They also reported that the amount of CO and CO_2 in the O_2 pulse was strongly influenced by the C_3H_8 pulse size; the larger the pulse size the larger the amount of CO_x formed. The formation of coke-like species over $VO_x(1/973\ K)/\gamma\text{-}Al_2O_3$ was observed in our previous *in situ* UV/Vis study of the reduction of VO_x species with propane.[26] No formation of such species was detected over samples with higher vanadium loading. The coke formation was related to the polymerisation of propene on acidic sites on bare γ-Al_2O_3 surfaces.

At all time delays, propene transient responses were observed immediately after propane followed by the transient responses of formaldehyde and CO_x. The same order of appearance of these reaction products was observed after single pulses of propane or propene (Fig. 2). The degrees of propane conversion upon sequential pulsing of O_2 and C_3H_8 over $VO_x(9.5/973)/\gamma\text{-}Al_2O_3$ at 773 K for different time delays (Δt = 0–1 s) are compared in Fig. 4. No dependence (increase or decrease) of the degree of propane conversion on the time delay between the O_2 and C_3H_8 pulses could be identified. From this result it can be concluded that no adsorbed oxygen species take part in propane activation under the applied experimental conditions, but the lattice oxygen does. Since MS analysis is not appropriate for precise CO and CO_2 analysis in the presence of C_3H_8 due to overlapping of the MS spectra, no strong conclusions on the participation of adsorbed oxygen species in CO_x formation could be derived from these experiments. In order to overcome this drawback, the oxygen isotope $^{18}O_2$ was used in the sequential pulsing of oxygen and propane. No ^{18}O was observed in CO_x for any of the catalysts. Based on the absence of ^{18}O in CO_x it is concluded that only lattice oxygen from VO_x takes part in the formation of CO_x under the conditions applied. This conclusion is also supported by the results of pulsing an oxygen–propane ($^{18}O_2/C_3H_8$ = 0.5) mixture: only $C^{16}O$, $C^{16}O_2$ and $H_2C^{16}O$ were formed. The absence of labelled (^{18}O) oxygen in CO_x can be explained by the fact that during the pulsing process gas phase $^{18}O_2$ was only consumed for catalyst regeneration; *i.e.* it was dissolved in a very large reservoir of ^{16}O lattice oxygen. Additionally, no scrambled oxygen $^{18}O^{16}O$ was observed when $^{18}O_2$ was pulsed over VO_x/γ-Al_2O_3. Only $^{18}O_2$ and $^{16}O_2$ were detected at the reactor outlet. This is due to the fact that the amount of $^{18}O_2$ pulsed is

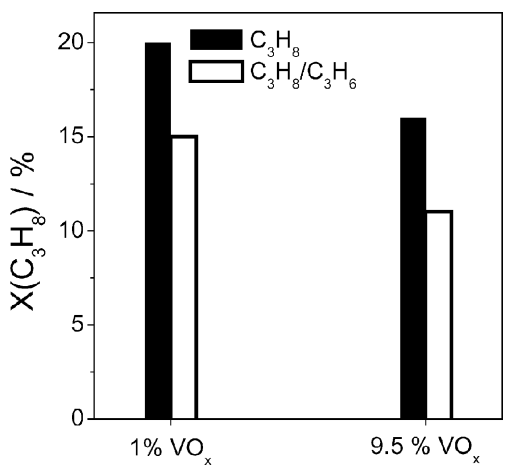

Fig. 3 Degree of propane conversion over $VO_x(1/973)/\gamma\text{-}Al_2O_3$ and $VO_x(9.5/973)/\gamma\text{-}Al_2O_3$ upon pulsing C_3H_8 : Ne = 1 : 1 (black bars) and C_3H_8 : C_3H_6 : Ne = 10 : 1 : 10 (open bars) mixtures at 773 K.

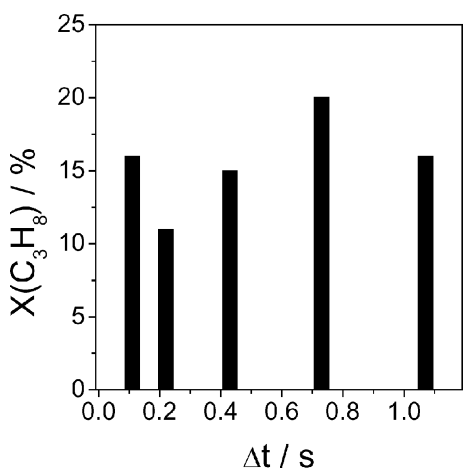

Fig. 4 Degree of propane conversion as a function of the time delay between pulsing O_2/Xe = 1 and C_3H_8/Ne = 1 mixtures at 773 K.

considerably lower than the amount of ^{16}O in VO_x species. Therefore, from a statistical point of view, the recombination of two ^{16}O atoms is favoured over recombination of ^{16}O and ^{18}O. Only an exchanged oxygen isotope ($^{16}O_2$) appeared in the $^{18}O_2$ pulse experiments; this indicates that oxygen chemisorption is irreversible. This agrees well with previously reported results on the ODP reaction over VO_x/ZrO_2[17] and complex vanadium-based oxide catalysts.[31]

3.3.3 Reducibility of VO_x species. To gain fundamental insights into the reducibility of different VO_x species and the effect of the reduction state of these sites on product distribution in the ODP reaction, selected VO_x/γ-Al_2O_3 materials were progressively treated by pulses containing a large number (*ca.* 10^{16}) of C_3H_8 molecules. Propane conversion, product selectivity and the ratio of removed oxygen species ($O_{removed}$) to the total number of V atoms (V_{total}) were determined. For $VO_x(4.6/873\ K)/\gamma$-Al_2O_3 and $VO_x(9.5/973\ K)/\gamma$-Al_2O_3, the catalytic performance is exemplified in Fig. 5. At the very beginning low selectivity towards propene (15–20%) was obtained for all of the catalytic materials studied at a degree of propane conversion of between 15–25%. Generally, with an increase in the ratio of $O_{removed} : V_{total}$ the degree of propane conversion decreases while propene selectivity increases (Fig. 5(a)). Similar results have been obtained previously for the ODP reaction over VO_x/TiO_2[32] and V–Mg–O[23] catalytic materials under transient oxygen-free conditions. The $VO_x(9.5/973\ K)/\gamma$-Al_2O_3 sample is the only example in which the propane conversion and propene selectivity stay on the same level with an increasing ratio of $O_{removed} : V_{total}$.

It is possible that the low initial selectivity towards propene is due to a very high concentration of near-surface lattice oxygen compared to the amount of propane pulsed. This results in a high initial conversion of propane to propene followed by a fast consecutive oxidation to CO_x. With progressive propane pulsing, the concentration of lattice oxygen decreases due to its removal for propane/propene oxidation. Therefore, the concentration of active lattice oxygen on the catalyst surface is expected to reduce, resulting in the isolation of active oxygen species from each other. In turn, the non-selective oxidation of propene to CO_x is inhibited because more than one neighbouring lattice oxygen is necessary for CO_x formation. The constant propane conversion and low propene selectivity over $VO_x(9.5/973)/\gamma$-Al_2O_3 in Fig. 5(b) can be explained in the following way. As experimentally proven by XRD analysis, this sample possesses bulk-like V_2O_5 (Table 1). Taking into account the apparent surface density of 129 V nm^{-2} for the vanadium species in Table 1 and the value of 10 V nm^{-2} for a vanadium monolayer,[2] the ratio of surface to bulk vanadium is roughly estimated as 0.08, *i.e.* less than 10% of total vanadium is on the catalyst surface. If only surface VO_x species participate in oxygen-free propane oxidation, the ratio of $O_{removed} : V_{total}$ would not exceed 0.1, which corresponds to the reduction of V_2O_5 to V_2O_3. However, the experimentally determined value of $O_{removed} : V_{total}$ in Fig. 5(b) is 0.2. Based on the above discussion, the high stability of $VO_x(9.5/973)/\gamma$-Al_2O_3 for oxygen-free propane oxidation can only be explained by a reoxidation of the active surface VO_x species *via* a migration of lattice oxygen within the bulk-like

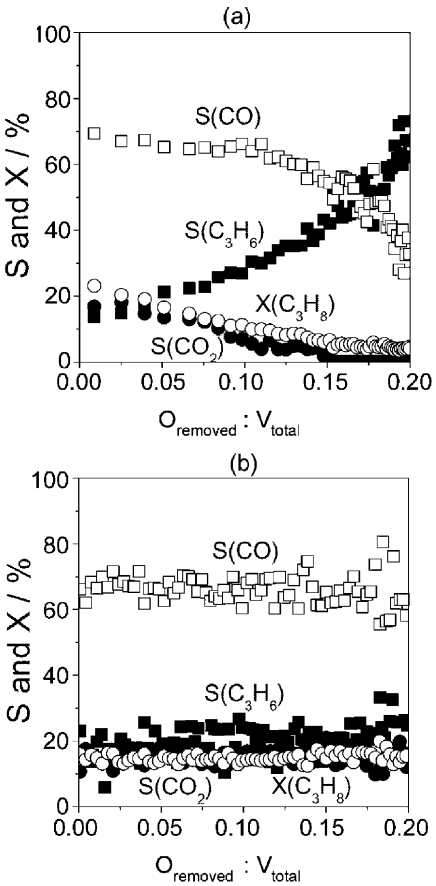

Fig. 5 Propane conversion and products selectivity *vs* the ratio of $O_{removed} : V_{total}$ upon C_3H_8 pulsing over (a) $VO_x(4.5/873)/\gamma$-Al_2O_3 and (b) $VO_x(9.5/973)/\gamma$-Al_2O_3 at 773 K.

V_2O_5. This agrees with previous studies of the ODP reaction over VMgO catalysts.[33]

In order to find out whether the reduction of VO_x species by propane depends on their structure, the normalised propane conversion (the degree of propane conversion in each propane pulse divided by that in the first pulse) was calculated and plotted against the ratio of $O_{removed} : V_{total}$ (Fig. 6). It is clear

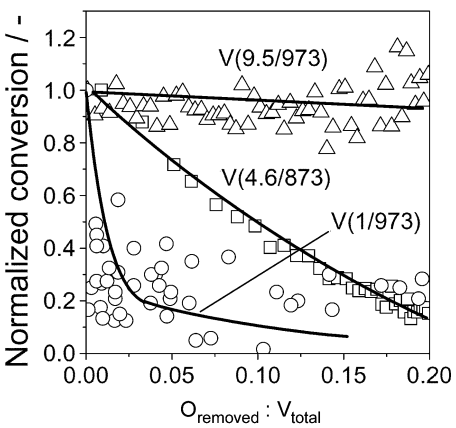

Fig. 6 Normalised propane conversion over different VO_x/γ-Al_2O_3 materials *vs* the ratio of $O_{removed} : V_{total}$ upon C_3H_8 pulsing at 773 K.

that the amount of lattice oxygen, which can be removed from differently structured VO_x species, increases in the order: highly dispersed VO_x species < polymerised VO_x species < bulk-like V_2O_5. Based on these observations, it can be said that the lower the vanadium loading, the lower the reactivity of lattice oxygen in partially reduced catalysts for propane oxidation. The lower activity of highly dispersed VO_x species compared to polymerised ones correlates well with the activity order of these two types of VO_x species in the ODP reaction (Table 2), *i.e.* the lower the reducibility, the lower the catalytic activity.

3.3.4 Mechanistic insights into the interaction of propene with VO_x/γ-Al_2O_3. Height-normalised transient responses of propene over selected catalysts at 573 K are presented in Fig. 7(a). The normalised transient responses differ significantly in their form. This may be due to the different activities of the VO_x/γ-Al_2O_3 materials towards propene adsorption/desorption or further transformation to CO_x. In order to discriminate between reversible and irreversible chemical processes, normalised experimental transient responses of propene were compared with the standard diffusion curve determined according to the procedure described in ref. 28. The results for three selected catalysts are presented in Fig. 7(b). It is obvious that the normalised transient response of propene over $VO_x(4.5/973)/\gamma$-Al_2O_3 is smaller than, and does not cross, the transient response of the inert gas, where only diffusion takes place. This is also valid for $VO_x(9.5/973)/\gamma$-Al_2O_3 and $VO_x(9.5/873)/\gamma$-Al_2O_3 catalysts. Based on ref. 28, the results presented in Fig. 7(b) let us conclude that propene reacts oxidatively over the above materials. In contrast to these catalysts, the normalised transient responses of propene over $VO_x(1/973\ K)/\gamma$-Al_2O_3 and $VO_x(4.5/873\ K)/\gamma$-Al_2O_3 (Fig. 7(b)) cross the standard diffusion curve. This means that in addition to the above reaction, propene adsorbs reversibly.

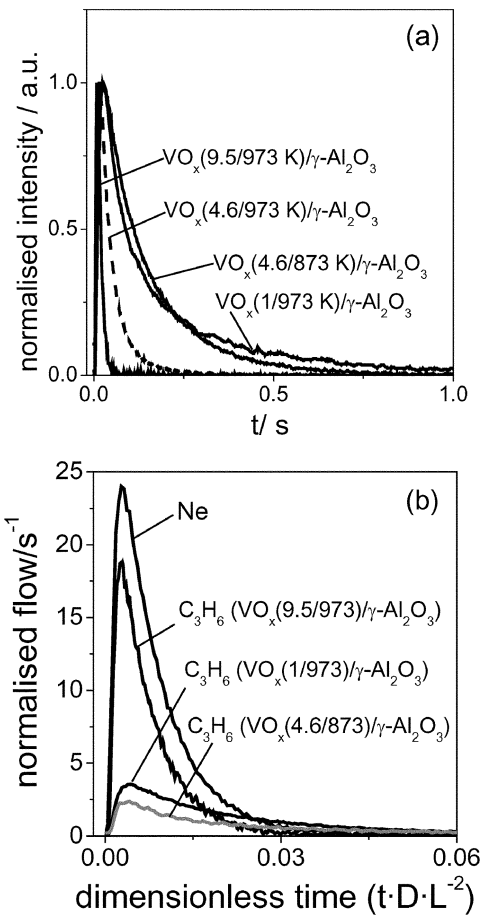

Fig. 7 (a) Height-normalised and (b) normalised according to ref. 28 propene transient responses over different catalysts at 573 K.

Considering the above mechanistic insights into propene interaction with the materials studied, they can be divided into two groups: i) $VO_x(1/973\ K)/\gamma$-Al_2O_3 and $VO_x(4.5/873\ K)/\gamma$-Al_2O_3 and ii) $VO_x(4.6/973\ K)/\gamma$-Al_2O_3, $VO_x(9.5/973\ K)/\gamma$-Al_2O_3 and $VO_x(9.5/873\ K)/\gamma$-Al_2O_3. Propene strongly adsorbs and slowly desorbs from materials of the first group. Based on the apparent surface densities of vanadium presented in Table 1, it is expected that VO_x species over $VO_x(1/973)/\gamma$-Al_2O_3 and $VO_x(4.5/873)/\gamma$-Al_2O_3 do not completely cover all parts of the bare γ-Al_2O_3 surface, which is a well-known acidic support.[7] Usually, catalyst acidity is measured by means of adsorption/desorption of probe molecules such as ammonia or pyridine. These molecules are of basic nature due to the presence of an unbound electron pair. The propene molecule possesses a double bond, which also provides a basic character. Therefore, propene adsorption/desorption may reflect the acidic properties of solid materials. According to the above discussion, the catalyst acidity is considered to be the reason for the differences in propene interaction with differently loaded VO_x/γ-Al_2O_3 (Fig. 7).

3.4 Mechanistic network of the ODP reaction

The results of present transient and steady state studies as well as those of previous catalyst characterisation[26,27] are discussed together, in order to elaborate structure–selectivity relationships in the ODP reaction over VO_x/γ-Al_2O_3 materials possessing differently structured VO_x species. The relationships between product selectivity and C_3H_8 conversion show (see Fig. 1) that propane is initially oxidised to propene followed by its consecutive oxidation to CO_x. The degree of polymerisation of the VO_x species strongly influences the non-selective consecutive propene oxidation; the higher the degree of polymerisation, the more significant is this reaction pathway. However, direct oxidation of C_3H_8 to CO_x is inhibited over polymerised VO_x species and bulk-like V_2O_5 compared to highly dispersed VO_x species (Table 2). A similar effect of vanadium loading (apparent density of surface VO_x species) on initial propene selectivity was reported for VO_x/ZrO_2.[19,34]

Considering the presence of a partly bare γ-Al_2O_3 surface, the following mechanistic concept of the ODP reaction (Fig. 8) is suggested. Propane is activated over VO_x species yielding a surface intermediate, which is stabilized in the vicinity of acidic sites on bare areas of the support. This intermediate can be transformed to C_3H_6, or further oxidised to CO and CO_2 in parallel according to the reaction pathways j_{6+}, j_2 and j_3, respectively. The formation of C_3H_6, CO and CO_2 from the same surface intermediate would explain the apparent primary nature of these reaction products over $VO_x(1/973)/\gamma$-Al_2O_3

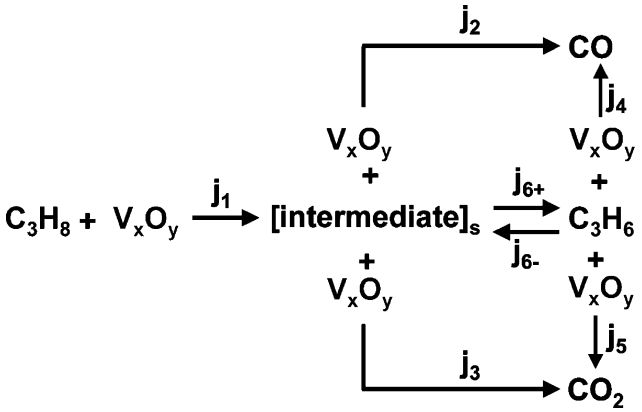

Fig. 8 Suggested reaction scheme of propane oxidation.

and $VO_x(4.5/873)/\gamma$-Al_2O_3 (Fig. 1). With a further increase in vanadium loading (*i.e.*, a decreasing concentration of bare support sites) j_{6+} will prevail over j_{6-}, j_2 and j_3 resulting in a decrease in the contribution of apparent CO_x formation from propane but in an increase in consecutive propene oxidation to CO (j_4) and CO_2 (j_5) over VO_x species. Evans *et al.*[35] similarly discussed the effect of apparent surface VO_x density on initial propene selectivity over $VO_x/MgAl_2O_3$. These authors found that the contribution of direct propane conversion to CO_x decreases with an increase in the apparent surface density of VO_x species. The decrease in this ratio was explained by the blocking of non-selective bare $MgAl_2O_4$ sites with selective VO_x species.

The highest initial propene selectivity is predicted to occur over the catalyst completely covered by VO_x species, since propene adsorption over acidic bare sites of the support is strongly suppressed. Experimental results in Fig. 1 and Table 2 support this conclusion. However, the density of lattice oxygen species at full surface coverage by VO_x species highly favours consecutive propene oxidation to CO_x.

To achieve a high catalyst performance in the ODP reaction it appears desirable to design catalytic surfaces which are completely covered by well-dispersed vanadia species to avoid the strong adsorption of propene on the support surface. Moreover, the surface density of active lattice oxygen should also be optimised. The possibility of tailoring the concentration of the active oxygen species to a required amount was recently demonstrated by our group for the ODP reaction over VO_x/MCM-41[36] and VO_x/γ-Al_2O_3[26] catalysts using N_2O as a "mild" oxidant. Propene selectivity could be increased by *ca.* 20% compared to an O_2-containing reaction feed. From measurements of contact potential differences, N_2O was shown to reoxidise reduced VO_x species over VO_x/γ-Al_2O_3 slower than O_2.[26] Moreover, *in situ* UV/Vis analysis, which was carried out under the ODP reaction conditions with either O_2 or N_2O revealed that the average oxidation state of vanadium is lower in the presence of N_2O than O_2. Thus, due to the fact that N_2O is less able to reoxidise reduced VO_x species than O_2, steady state coverage by active lattice oxygen is lower than in the presence of O_2. However, from a practical point of view, the use of N_2O as an oxidant for the ODP reaction does not seem to be relevant. This situation may be changed if N_2O becomes more readily available in sufficient quantities.

4 Summary

A mechanistic investigation of the ODP reaction by means of steady state and transient mechanistic experiments was performed over VO_x/γ-Al_2O_3 catalysts possessing highly dispersed, polymerised VO_x species and bulk-like V_2O_5. Based on the results of the transient experiments in the TAP reactor, propene is primarily formed from propane *via* oxidative dehydrogenation by lattice oxygen of VO_x species and not by adsorbed oxygen species. Propene is further oxidised to CO and CO_2. Formaldehyde was found to be an intermediate of the non-selective oxidation of C_3H_6 to CO_x; lattice oxygen of VO_x species breaks a C–C bond in the propene molecule yielding formaldehyde. This general reaction scheme is valid for differently structured VO_x species.

From steady state tests at ambient pressure, the following order of the initial propene selectivity (at zero degree of propane conversion) over differently structured VO_x species was established: bulk-like V_2O_5 > polymerised VO_x > highly dispersed VO_x species. Bulk-like V_2O_5 shows the highest initial propene selectivity of *ca.* 100%. The low selectivity of highly dispersed VO_x species is due to the fact that these species do not fully cover the acidic sites of the γ-Al_2O_3 support where propene adsorption and its further non-selective oxidation take place. Upon progressing from highly dispersed VO_x species to bulk-like V_2O_5, the bare γ-Al_2O_3 surface is completely covered by VO_x species and propene adsorption decreases; this results in very high initial propene selectivity. However, this high selectivity of bulk-like V_2O_5 decreases strongly with an increase in the degree of propane conversion due to a high density of neighbouring VO_x species, which offer sufficient oxygen for the consecutive reactions to CO_x. This decrease in propene selectivity is influenced by the structure of VO_x species. Highly dispersed VO_x species have the lowest ability for consecutive propene oxidation to CO_x.

Acknowledgements

Support by Deutsche Forschungsgemeinschaft (DFG) within the framework of the competence network (Sonderforschungsbereich 546) "Structure, dynamics and reactivity of transition metal oxide aggregates" has been greatly appreciated.

References

1 E. A. Mamedov and V. C. Corberan, *Appl. Catal., A*, 1995, **127**, 1.
2 T. Blasco and J. M. López Nieto, *Appl. Catal., A*, 1997, **157**, 117.
3 O. V. Buyevskaya and M. Baerns, *Catalysis*, 2002, **16**, 155.
4 M. Baerns, G. Grubert, E. V. Kondratenko, D. Linke and U. Rodemerk, *Oil Gas-Eur. Mag.*, 2003, **1**, 36.
5 F. Cavani and F. Trifiró, *Catal. Today*, 1997, **36**, 431.
6 R. K. Grasselli, *Catal. Today*, 1999, **49**, 141.
7 J. Le Bars, A. Auroux, M. Forissier and J. C. Vedrine, *J. Catal.*, 1996, **162**, 250.
8 M. M. Koranne, J. G. Goodwin and G. Marcelin, *J. Catal.*, 1994, **148**, 369.
9 J. M. Lopez Nieto, J. Soler, P. Concepcion, J. Herguido, M. Menendez and J. Santamaria, *J. Catal.*, 1999, **185**, 324.

10 J. M. Kanervo, M. E. Harlin, A. O. I. Krause and M. A. Banares, *Catal. Today*, 2003, **78**, 171.
11 J. G. Eon, R. Olier and J. C. Volta, *J. Catal.*, 1994, **145**, 318.
12 X. Gao and I. E. Wachs, *J. Phys. Chem. B*, 2000, **104**, 1261.
13 M. Machli, E. Heracleous and A. A. Lemonidou, *Appl. Catal., A*, 2002, **236**, 23.
14 F. Arena, N. Giordano and A. Parmaliana, *J. Catal.*, 1997, **167**, 66.
15 A. Khodakov, B. Olthof, A. T. Bell and E. Iglesia, *J. Catal.*, 1999, **181**, 205.
16 J. L. Male, H. G. Niessen, A. T. Bell and T. D. Tilley, *J. Catal.*, 2000, **194**, 431–444.
17 K. Chen, A. Khodakov, J. Yang, A. T. Bell and I. E., *J. Catal.*, 1999, **186**, 325–333.
18 K. Chen, A. T. Bell and E. Iglesia, *J. Phys. Chem. B*, 2000, **104**, 1292.
19 M. D. Argyle, K. Chen, A. T. Bell and E. Iglesia, *J. Catal.*, 2002, **208**, 139.
20 R. Grabowski, J. Sloczyñski and N. M. Grzesik, *Appl. Catal., A*, 2002, **232**, 277.
21 E. V. Kondratenko, M. Cherian and M. Baerns, *Catal. Today*, 2005, **99**, 59.
22 S. L. T. Andersen, *Appl. Catal., A*, 1994, **112**, 209.
23 A. Pantazidis, S. A. Bucholz, H. W. Zanthoff, Y. Schuurman and C. Mirodatos, *Catal. Today*, 1998, **40**, 207.
24 A. Bielanski and J. Haber, *Oxygen in Catalysis*, Marcel Dekker, New York, 1991, p. 320.
25 K. Chen, E. Iglesia and A. T. Bell, *J. Catal.*, 2000, **192**, 197–203.
26 E. V. Kondratenko and M. Baerns, *Appl. Catal., A*, 2001, **222**, 133.
27 N. Steinfeldt, D. Muller and H. Berndt, *Appl. Catal., A*, 2004, **272**, 201.
28 J. T. Gleaves, G. S. Yablonsky, P. Phanawadee and Y. Schuurman, *Appl. Catal., A*, 1997, **160**, 55.
29 G. Centi, *Appl. Catal., A*, 1996, **147**, 267.
30 G. Mul, M. A. Banares, G. Garcia Gortez, B. van der Linden, S. J. Khatib and J. A. Moulijn, *Phys. Chem. Chem. Phys.*, 2003, **5**, 4378.
31 E. V. Kondratenko, O. V. Buyevskaya and M. Baerns, *Top. Catal.*, 2001, **15**, 175.
32 O. V. Buyevskaya and M. Baerns, *Catal. Today*, 1998, **42**, 315.
33 H. W. Zanthoff, J. C. Jalibert, Y. Schuurman, P. Slama, J. M. Herrmann and C. Mirodatos, *Stud. Surf. Sci. Catal.*, 2000, **130**, 761.
34 C. Pak, A. T. Bell and T. D. Tilley, *J. Catal.*, 2002, **206**, 49.
35 O. R. Evans, A. T. Bell and T. D. Tilley, *J. Catal.*, 2004, **226**, 292.
36 E. V. Kondratenko, M. Cherian, M. Baerns, X. Su, R. Schlögl, X. Wang and I. E. Wachs, *J. Catal.*, 2005, **234**, 131.